Cell Reports Medicine, Volume *4*

Supplemental information

Tumor heterogeneity and tumor-microglia interactions in primary and recurrent IDH1-mutant gliomas

Enrique Blanco-Carmona, Ashwin Narayanan, Inmaculada Hernandez, Juan C. Nieto, Marc Elosua-Bayes, Xueyuan Sun, Claudia Schmidt, Necmettin Pamir, Koray Özduman, Christel Herold-Mende, Francesca Pagani, Manuela Cominelli, Julian Taranda, Wolfgang Wick, Andreas von Deimling, Pietro Luigi Poliani, Michael Rehli, Matthias Schlesner, Holger Heyn, and Şevin Turcan

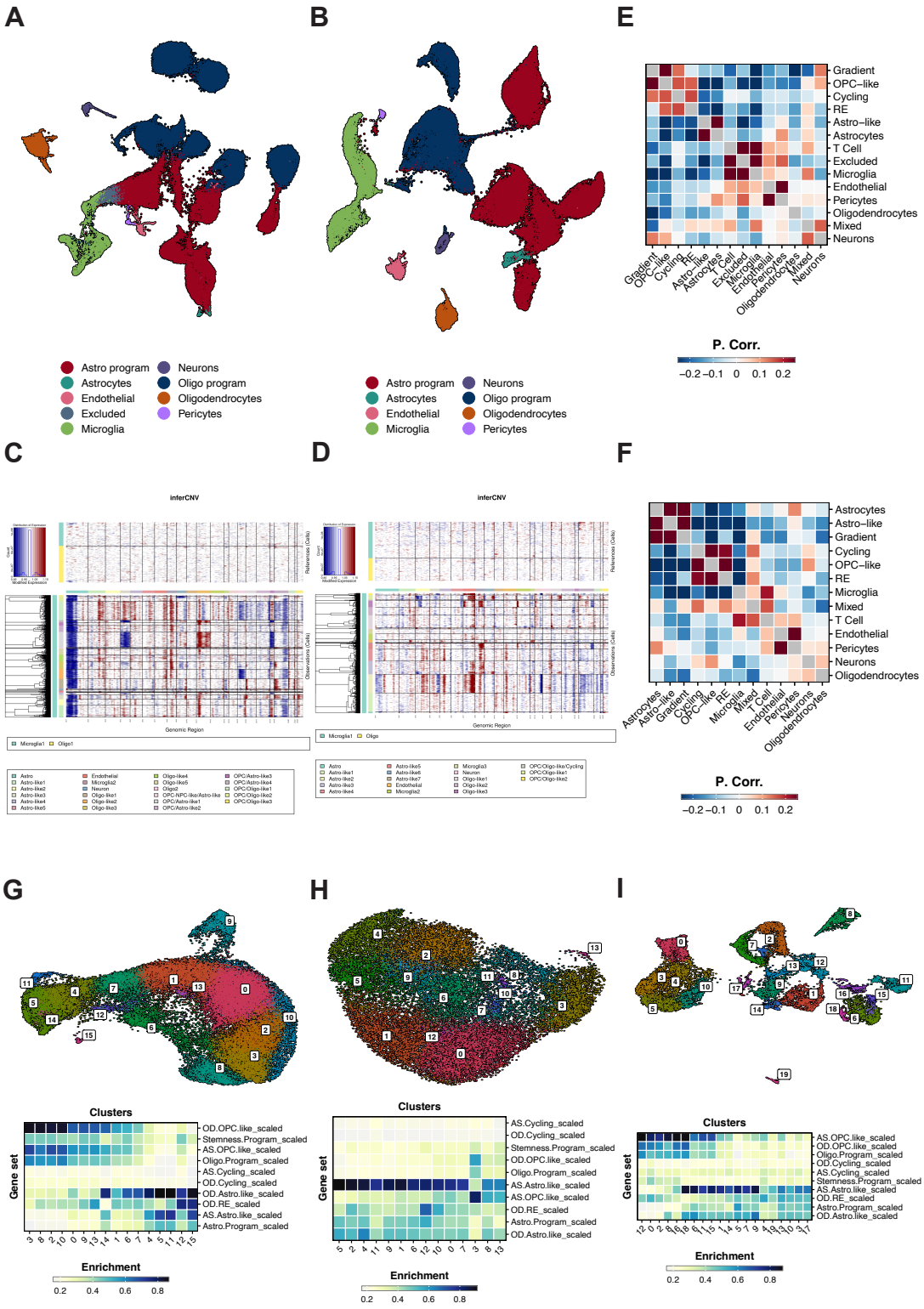
A
B
E
Astro program
Astrocytes
Endothelial
Excluded
Microglia
Neurons
Oligo program
Oligodendrocytes
Pericytes
Gradient
OPC−like
Cycling
RE
Astro−like
Astrocytes
T Cell
Excluded
Microglia
Endothelial
Pericytes
Oligodendrocytes
Mixed
Neurons
P. Corr.
−0.2 −0.1 0 0.1 0.2
C
D
F
inferCNV
Genomic Region
Microglia1
Oligo1
Oligo
Astrocytes
Astro−like
Gradient
Cycling
OPC−like
RE
Microglia
Mixed
T Cell
Endothelial
Pericytes
Neurons
Oligodendrocytes
G
H
I
Clusters
Gene set
OD.OPC.like_scaled
Stemness.Program_scaled
AS.OPC.like_scaled
Oligo.Program_scaled
AS.Cycling_scaled
OD.Cycling_scaled
OD.Astro.like_scaled
OD.RE_scaled
AS.Astro.like_scaled
Astro.Program_scaled
Enrichment
0.2 0.4 0.6 0.8

Figure S1. UMAP of merged snRNA-seq data, inferred CNVs, and characterization of the gradient cluster. Related to Figure 1 and STAR methods. (A and B) UMAP and initial cluster assignment for merged snRNA-seq data from oligodendroglioma **(A)** and astrocytoma **(B)**. Colors represent assigned cell types. UMAP1, *x*-axis; UMAP2, *y*-axis. **(C and D)** Heatmap of CNV profiles inferred from snRNA-seq from oligodendrogliomas **(C)** and astrocytomas **(D)**. Each row corresponds to a nucleus, ordered by initial cluster labeling from merged data. Red indicates gain and blue indicates loss. **(E and F)** Correlation heatmap depicting expression similarities (Pearson's correlation) between the highly variable genes in tumor and TME populations of oligodendrogliomas (**E**) and astrocytomas (**F**). **(G, H, and I)** Gradient subset of the tumor subpopulation for primary oligodendrogliomas (**G**), primary astrocytomas (**H**) and paired astrocytomas (**I**). Cells are re-normalized, and dimensional reduction is computed, generating a new UMAP embedding and clustering (top). For each cluster, enrichment scores for the NMF metaprograms and the programs described in *Venteicher, et al.* are computed, and displayed as an enrichment heatmap (bottom). UMAP1, *x*-axis; UMAP2, *y*-axis.

Figure S2

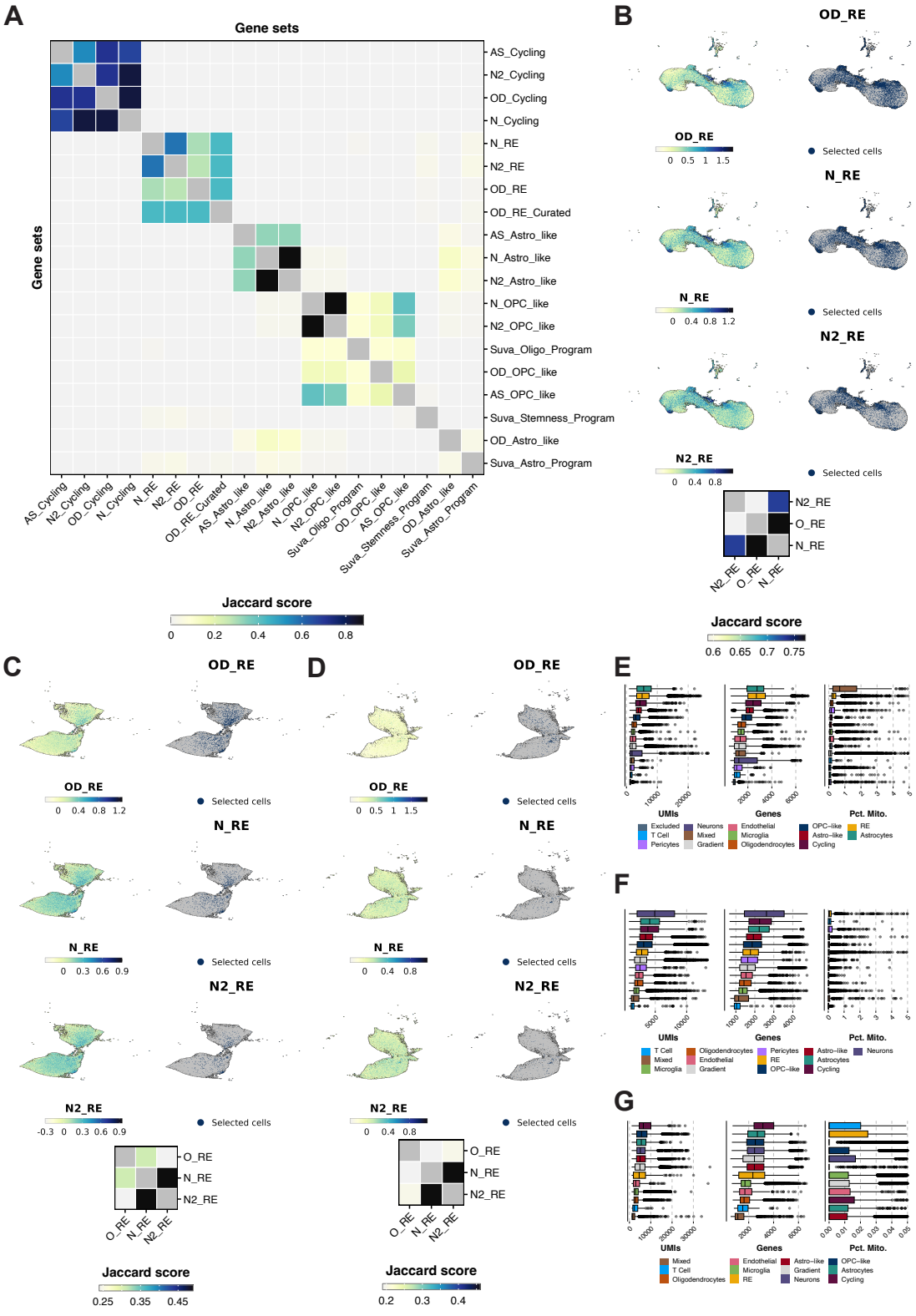
A
Gene sets
AS_Cycling
N2_Cycling
OD_Cycling
N_Cycling
N_RE
N2_RE
OD_RE
OD_RE_Curated
AS_Astro_like
N_Astro_like
N2_Astro_like
N_OPC_like
N2_OPC_like
Suva_Oligo_Program
OD_OPC_like
AS_OPC_like
Suva_Stemness_Program
OD_Astro_like
Suva_Astro_Program
Jaccard score
0 0.2 0.4 0.6 0.8
B
OD_RE
N_RE
N2_RE
Selected cells
O_RE
Jaccard score
0.6 0.65 0.7 0.75
C
D
E
F
G
UMIs
Genes
Pct. Mito.

Figure S2. **Characterization of the NMF programs, and quality control for all clusters in snRNA-seq datasets. Related to Figures 1 and 4, and STAR methods. (A)** Correlation matrix depicting the Jaccard similarities between the NMF metaprograms and the Astrocyte-like, Oligo-like and Stemness programs in *Venteicher, et al*. Three iterations of NMF have been computed, represented by the prefixes in the metaprograms name: OD_ and AS_ metaprograms belong to the first iteration, containing ribosomal genes. N_ metaprograms correspond to the metaprograms retrieved prior removal of ribosomal genes. N2_ metaprograms refer to the metaprograms retrieved prior removal of ribosomal genes and exclusion of sample *IDH_ACB_AD_540*, which has a significantly higher proportion of RE. OD_RE_Curated metaprogram contains the genes present in all three RE metaprogram iterations. (**B-D)** Jaccard similarities depict a high consensus between all homologue iterations of NMF metaprograms. Permutation testing selection method based on the enrichment scores for the three different RE metaprograms retrieved including ribosomal genes (*OD_RE*), excluding them (*N_RE*) and excluding the sample with the highest proportion of RE cells, *IDH_ACB_AD_540* (*N2_RE*) is used in the tumor cells of oligodendrogliomas (**B**) and astrocytomas (**C**) and paired astrocytomas **(D)**. Jaccard similarities between the selected cells for each of the NMF metaprograms is shown (bottom). Enrichment scores are shown on the left and the selected cells on the right. UMAP1, *x*-axis; UMAP2, *y*-axis. **(E-G)** Boxplots showing from left to right, distribution of UMIs per cell, genes per cell and percentage of mitochondrial RE per cell are shown for primary oligodendroglioma (**A**), primary astrocytoma (**B**) and paired astrocytoma (**C**) tumors.

Figure S3

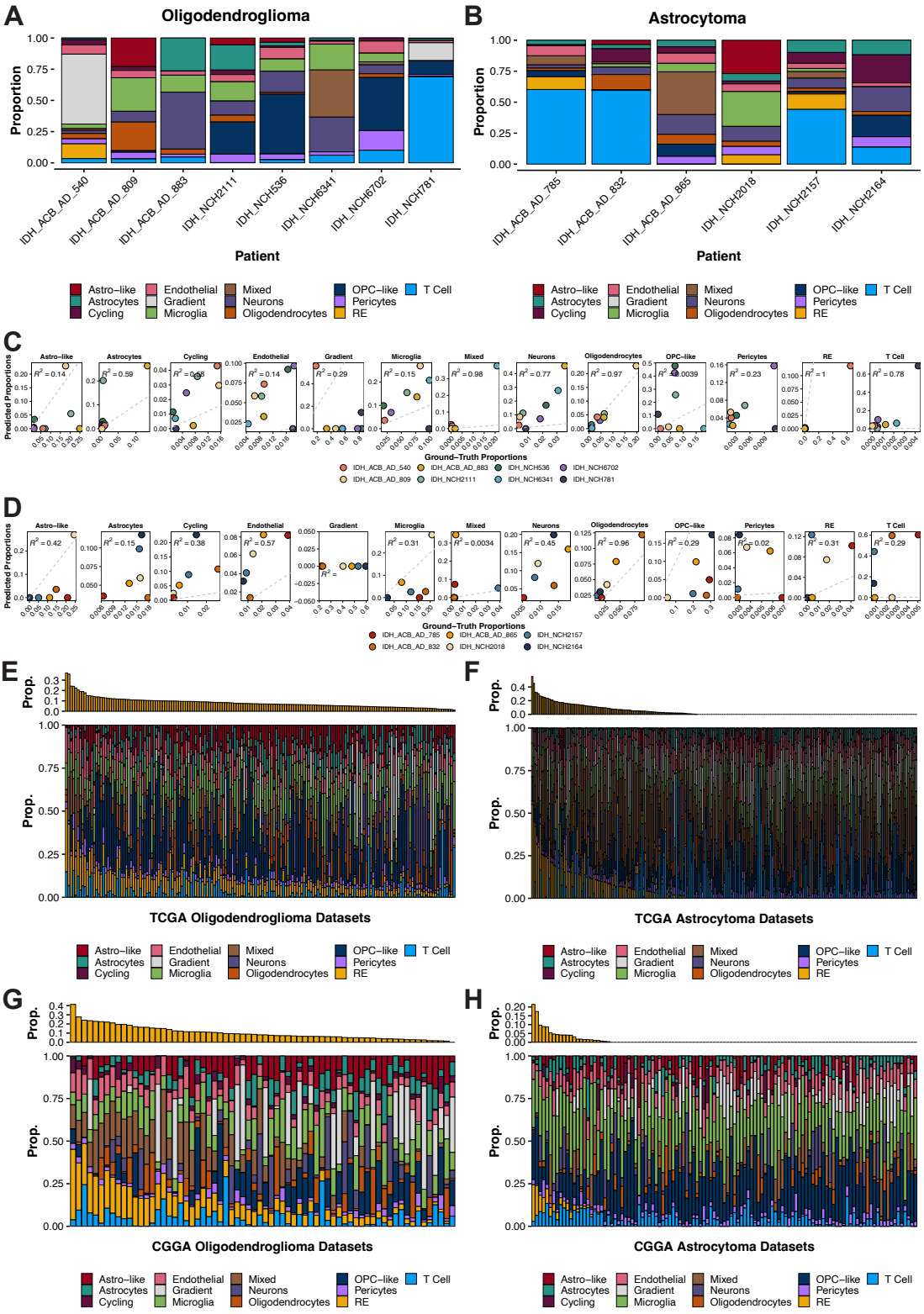
A
Oligodendroglioma
B
Astrocytoma
Proportion
Patient
IDH_ACB_AD_540
IDH_ACB_AD_809
IDH_ACB_AD_883
IDH_NCH2111
IDH_NCH536
IDH_NCH6341
IDH_NCH6702
IDH_NCH781
IDH_ACB_AD_765
IDH_ACB_AD_832
IDH_ACB_AD_865
IDH_NCH2018
IDH_NCH2157
IDH_NCH2164
Astro−like
Astrocytes
Cycling
Endothelial
Gradient
Microglia
Mixed
Neurons
Oligodendrocytes
OPC−like
Pericytes
RE
T Cell
C
D
Predicted Proportions
Ground−Truth Proportions
E
F
G
H
Prop.
TCGA Oligodendroglioma Datasets
TCGA Astrocytoma Datasets
CGGA Oligodendroglioma Datasets
CGGA Astrocytoma Datasets

Figure S3. **Deconvolution of publicly available bulk glioma RNA-seq datasets (TCGA and CGGA). Related to Figure 1 and STAR methods. (A)** Deconvolution of primary samples (pseudobulk) for oligodendroglioma (OD). **(B)** Deconvolution of primary samples (pseudobulk) for astrocytoma (AS). **(C)** Correlation analysis between predicted proportions (SPOTlight) ground-truth proportions (primary samples) in OD. **(D)** Correlation analysis between predicted proportions (SPOTlight) ground-truth proportions (primary samples) in AS. **(E)** SPOTlight results of TCGA (the Cancer Genome Atlas) OD IDH mutant glioma cohort (on top, proportion of RE, ordered. on the bottom, all proportions ordered also by descending RE). **(F)** SPOTlight results of TCGA AS IDH mutant glioma cohort (on top, proportion of RE, ordered. on the bottom, all proportions ordered also by descending RE) **(G)** SPOTlight results of CGGA OD (Chinese Glioma Genome Atlas) IDH mutant glioma cohort (on top, proportion of RE, ordered. on the bottom, all proportions ordered also by descending RE). **(H)** SPOTlight results of CGGA AS IDH mutant glioma cohort (on top, proportion of RE, ordered. on the bottom, all proportions ordered also by descending RE).

Figure S4

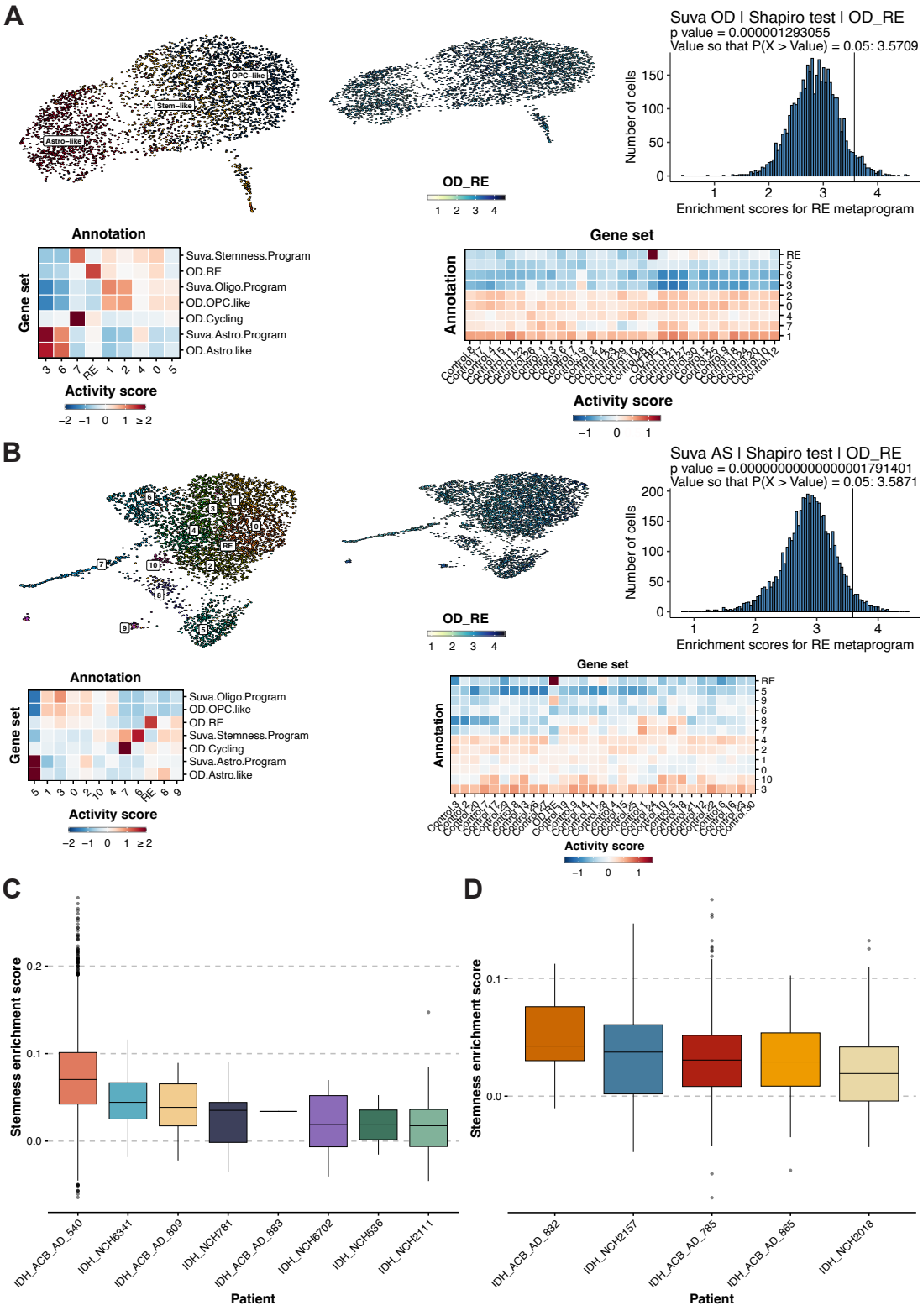
A
OPC−like
Stem−like
Astro−like
OD_RE
Suva OD I Shapiro test I OD_RE
p value = 0.000001293055
Value so that P(X > Value) = 0.05: 3.5709
Number of cells
Enrichment scores for RE metaprogram
Annotation
Gene set
Suva.Stemness.Program
OD.RE
Suva.Oligo.Program
OD.OPC.like
OD.Cycling
Suva.Astro.Program
OD.Astro.like
Activity score
B
Suva AS I Shapiro test I OD_RE
p value = 0.00000000000000001791401
Value so that P(X > Value) = 0.05: 3.5871
C
Stemness enrichment score
IDH_ACB_AD_540
IDH_NCH6341
IDH_ACB_AD_809
IDH_NCH781
IDH_ACB_AD_883
IDH_NCH6702
IDH_NCH536
IDH_NCH2111
Patient
D
IDH_ACB_AD_832
IDH_NCH2157
IDH_ACB_AD_785
IDH_ACB_AD_865
IDH_NCH2018

Figure S4. The RE metaprogram in publicly available scRNA-seq datasets from IDH mutant gliomas, and the stemness score per patient in snRNA-sq dataset from oligodendrogliomas and astrocytomas. Related to Figure 1 and STAR methods (A and B) Datasets from publicly available oligodendrogliomas[3] **(A)** and astrocytomas[4] **(B)** are used to determine the presence of the RE metaprogram. UMAP representation of the tumor cells is shown together with the enrichment scores for the RE metaprogram (top, left and middle). The distribution of enrichment scores is tested for normality using Shapiro test (top-right) and the value so that the probability of finding an enrichment score higher is 5% is used to select the RE population. The activity of the different cell clusters and the RE population towards the NMF metaprograms and the publicly available programs[4] is computed by using *decoupleR*. Activity scores are scaled and centered and displayed grouped by cell population (bottom-left). To query the robustness of RE metaprogram towards the RE population, 50 different gene sets of equal size are generated by randomly selecting genes in the same bin of expression as the genes in the RE metaprogram. Activity scores are computed, scaled, and centered, and displayed grouped by cell population. UMAP1, *x*-axis; UMAP2, *y*-axis. **(C and D)** Box plots of the enrichment score for the stemness program in *Venteicher, et al* per patient in oligodendroglioma (**C**) and astrocytoma (**D**).

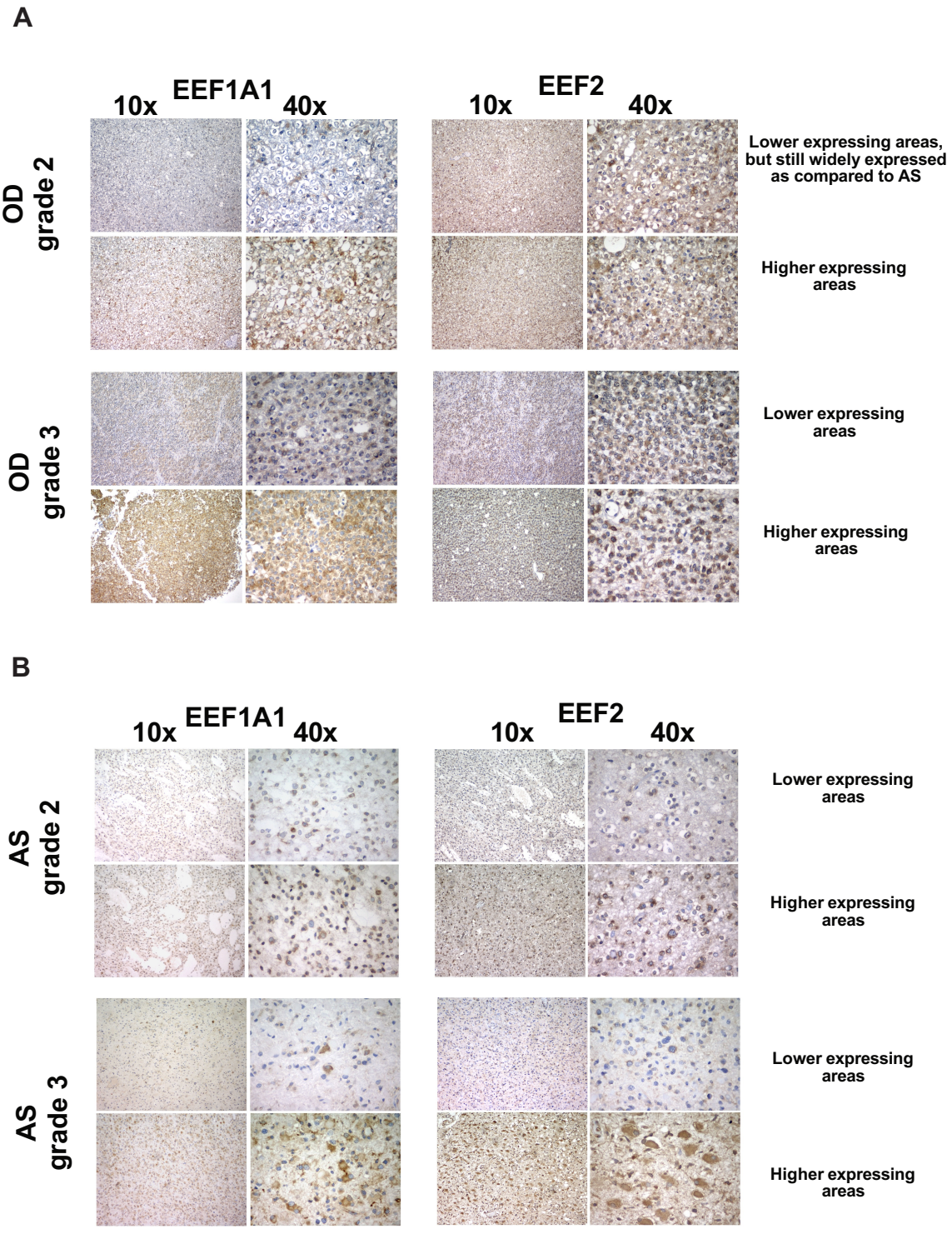

Figure S5. Representative IHC staining for EEF1A1 and eEF2 in IDH mutant gliomas. Relate to Figure 1. **(A, B)** Representative IHC staining for EEF1A1 and eEF2 population marker genes in grade 2 (top) and grade 3 (bottom) oligodendrogliomas **(A)** and astrocytomas **(B)**. Images are shown as 10x and 40x to show the spatial distribution of EEF1A1 and EEF2 in both tumor types. *OD*, oligodendroglioma; *AS*, astrocytoma.

Figure S6

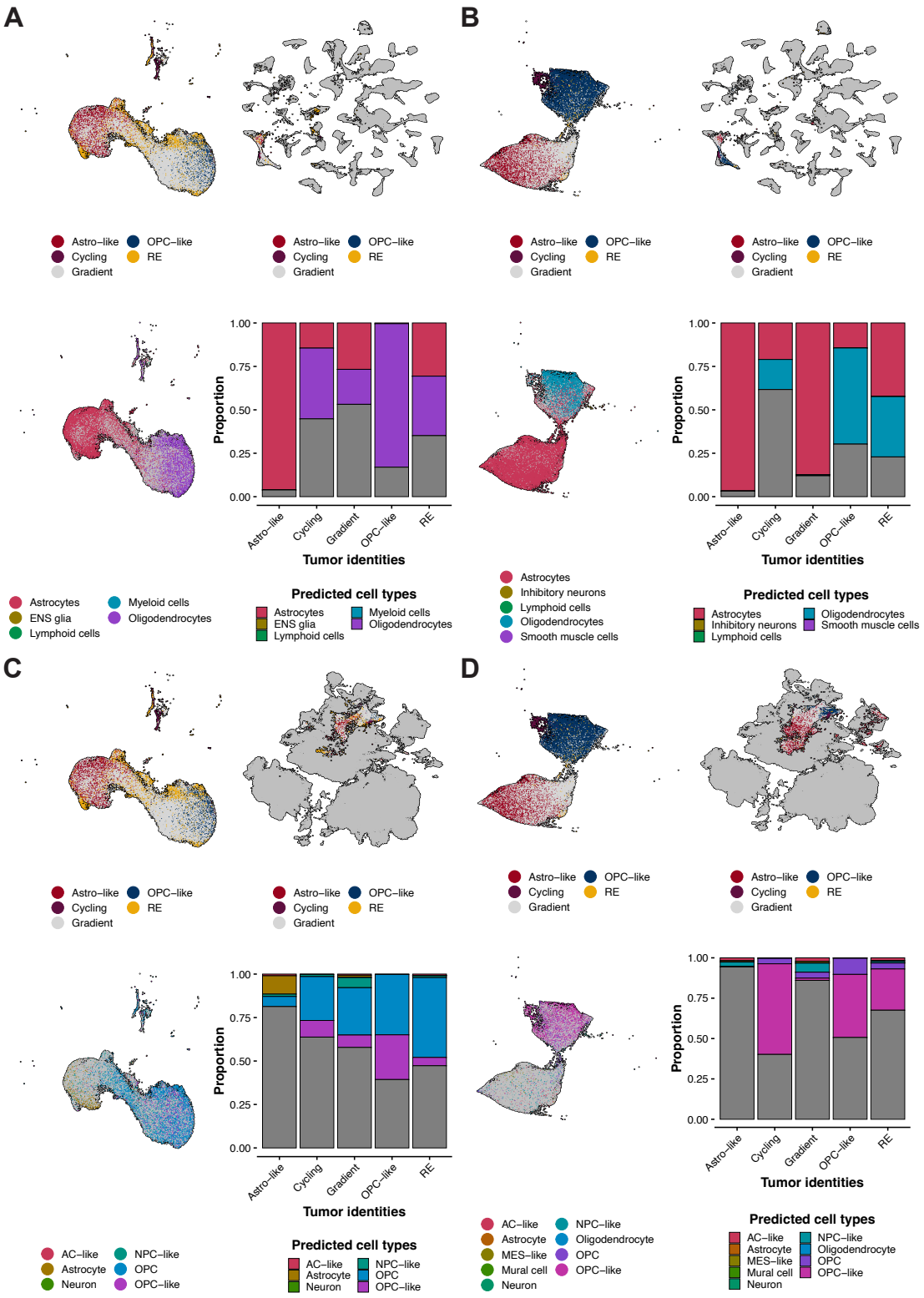
A
B
C
D
Astro–like
OPC–like
Cycling
RE
Gradient
Proportion
1.00
0.75
0.50
0.25
0.00
Astro–like
Cycling
Gradient
OPC–like
RE
Tumor identities
Predicted cell types
Astrocytes
ENS glia
Lymphoid cells
Myeloid cells
Oligodendrocytes
Inhibitory neurons
Smooth muscle cells
AC–like
Astrocyte
Neuron
NPC–like
OPC
MES–like
Mural cell
Oligodendrocyte

Figure S6. **Reference mapping using Azimuth. Related to Figure 1 and STAR methods. (A, B)** Tumor subsets for primary oligodendrogliomas **(A)** and primary astrocytomas **(B)** are mapped onto the *fetus reference* from Azimuth. **(C, D)** Tumor subsets for primary oligodendrogliomas **(C)** and primary astrocytomas **(D)** are mapped onto the *GBmap* reference. For each variation, original UMAP embedding is shown on the top-left, cells mapped onto the reference UMAP on the top-right, cells re-labelled based on the reference mapping on the bottom left and a bar plot of the proportions of the new annotation per each original tumor entity on the bottom-right. UMAP1, *x*-axis; UMAP2, *y*-axis.

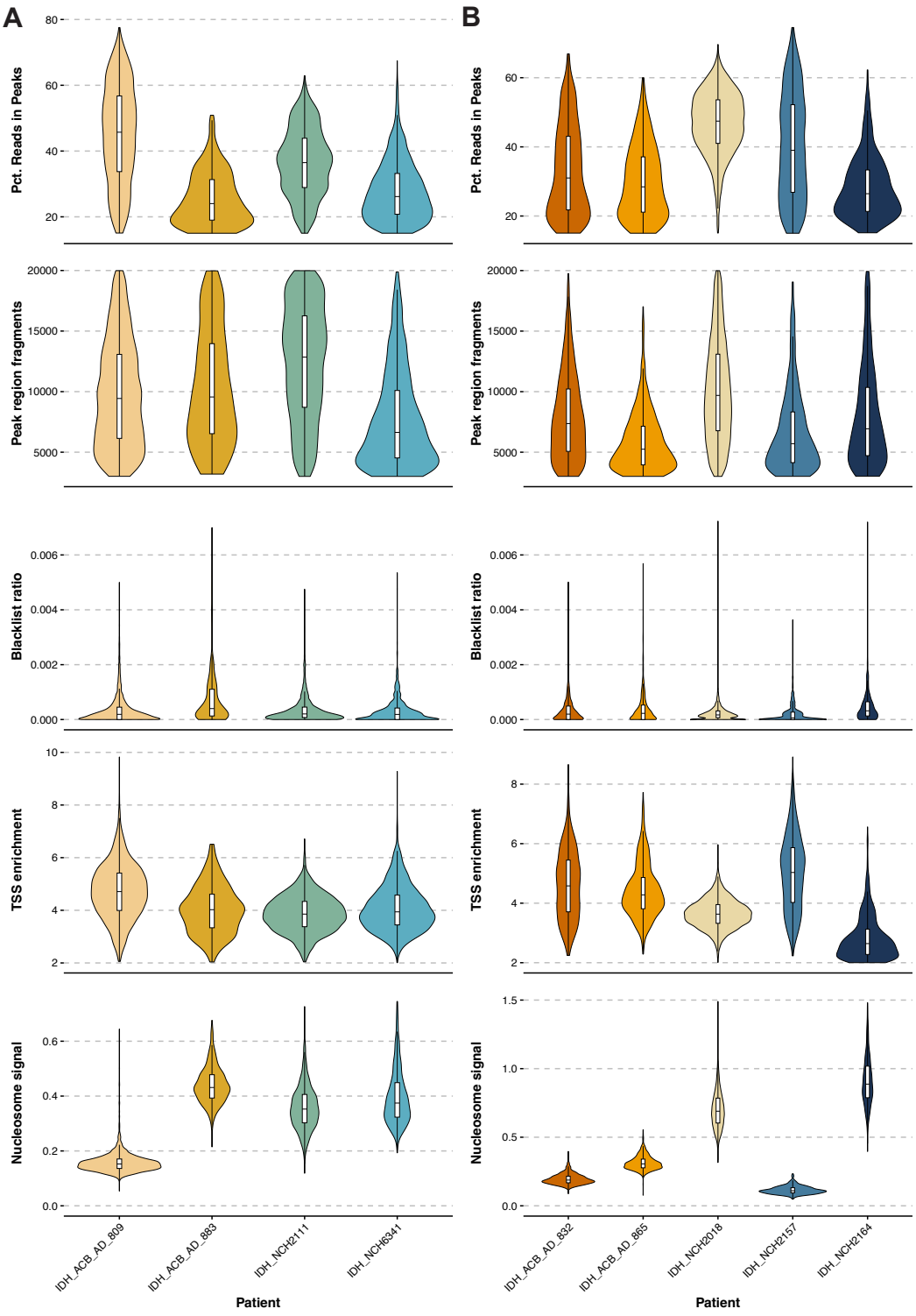

Figure S7. Quality control metrics of snATAC-seq data. Related to Figure 2. (A and B) Quality control metrics of snATAC-seq data generated from oligodendrogliomas **(A)** and astrocytomas **(B)**. From top to bottom: Percentage of reads in peaks; peak region fragments; blacklist ratio; transcription start site (TSS) enrichment score and nucleosome signal.

Figure S8

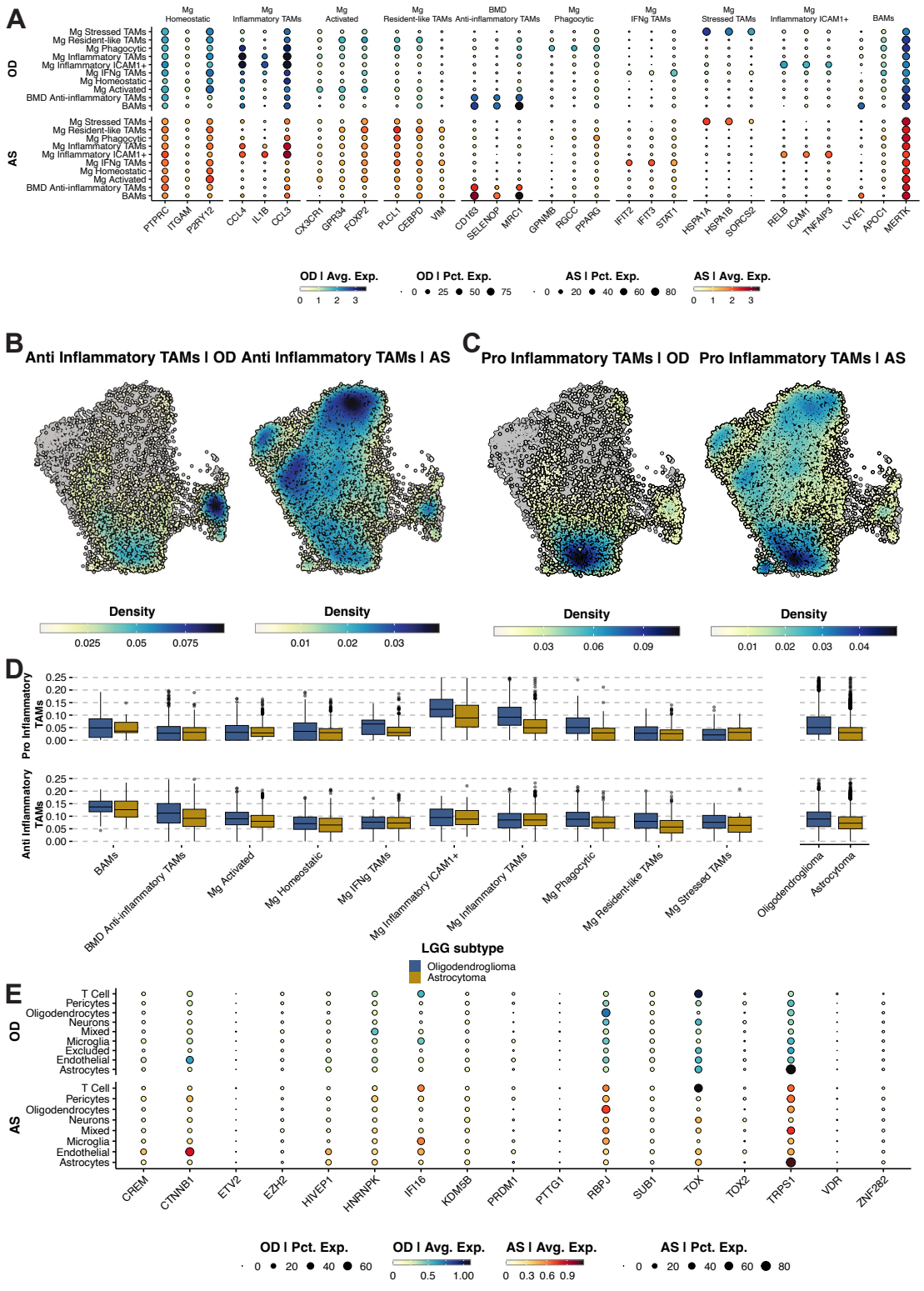
A
OD
AS
Mg Homeostatic
Mg Inflammatory TAMs
Mg Activated
Mg Resident-like TAMs
BMD Anti-inflammatory TAMs
Mg Phagocytic
Mg IFNg TAMs
Mg Stressed TAMs
Mg Inflammatory ICAM1+
BAMs
Mg Stressed TAMs
Mg Resident-like TAMs
Mg Phagocytic
Mg Inflammatory TAMs
Mg Inflammatory ICAM1+
Mg IFNg TAMs
Mg Homeostatic
Mg Activated
BMD Anti-inflammatory TAMs
BAMs
PTPRC
ITGAM
P2RY12
CCL4
IL1B
CCL3
CX3CR1
GPR34
FOXP2
PLCL1
CEBPD
VIM
CD163
SELENOP
MRC1
GPNMB
RGCC
PPARG
IFIT2
IFIT3
STAT1
HSPA1A
HSPA1B
SORCS2
RELB
ICAM1
TNFAIP3
LYVE1
APOC1
MERTK
OD | Avg. Exp.
0 1 2 3
OD | Pct. Exp.
0 25 50 75
AS | Pct. Exp.
0 20 40 60 80
AS | Avg. Exp.
0 1 2 3
B
Anti Inflammatory TAMs | OD
Anti Inflammatory TAMs | AS
Density
0.025 0.05 0.075
Density
0.01 0.02 0.03
C
Pro Inflammatory TAMs | OD
Pro Inflammatory TAMs | AS
Density
0.03 0.06 0.09
Density
0.01 0.02 0.03 0.04
D
Pro Inflammatory TAMs
Anti Inflammatory TAMs
0.25
0.20
0.15
0.10
0.05
0.00
BAMs
BMD Anti-inflammatory TAMs
Mg Activated
Mg Homeostatic
Mg IFNg TAMs
Mg Inflammatory ICAM1+
Mg Inflammatory TAMs
Mg Phagocytic
Mg Resident-like TAMs
Mg Stressed TAMs
Oligodendroglioma
Astrocytoma
LGG subtype
Oligodendroglioma
Astrocytoma
E
OD
AS
T Cell
Pericytes
Oligodendrocytes
Neurons
Mixed
Microglia
Excluded
Endothelial
Astrocytes
CREM
CTNNB1
ETV2
EZH2
HIVEP1
HNRNPK
IFI16
KDM5B
PRDM1
PTTG1
RBPJ
SUB1
TOX
TOX2
TRPS1
VDR
ZNF282
OD | Pct. Exp.
0 20 40 60
OD | Avg. Exp.
0 0.5 1.00
AS | Avg. Exp.
0 0.3 0.6 0.9
AS | Pct. Exp.
0 20 40 60 80

Figure S8. Markers for TAM subpopulations and TME of IDH mutant gliomas derived from snRNA-seq data. Related to Figure 1 and 3. (A) Dot plot showing three key marker genes for the TAM subpopulations in oligodendrogliomas (**top**) and astrocytomas (**bottom**). OD, oligodendroglioma; AS, astrocytoma. **(B)** Density gradient of pro-inflammatory and anti-inflammatory signatures in TAMs of astrocytomas **(B)** and oligodendrogliomas **(C)**. OD, oligodendroglioma; AS, astrocytoma. **(D)** Boxplots showing pro-inflammatory (top) and anti-inflammatory (bottom) scores per TAM subpopulation in oligodendrogliomas and astrocytomas. **(E)** Dot plot showing marker genes for the T cell population in oligodendrogliomas (top) and astrocytomas (bottom). OD, oligodendroglioma; AS, astrocytoma.

A

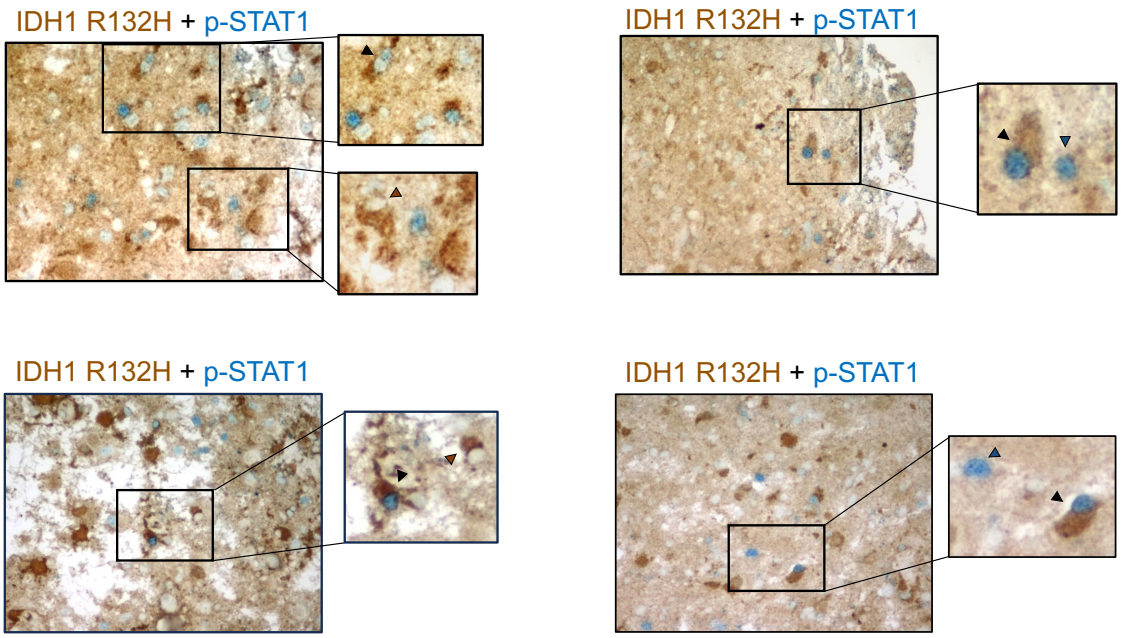
IDH1 R132H + p-STAT1
IDH1 R132H + p-STAT1
IDH1 R132H + p-STAT1
IDH1 R132H + p-STAT1

B

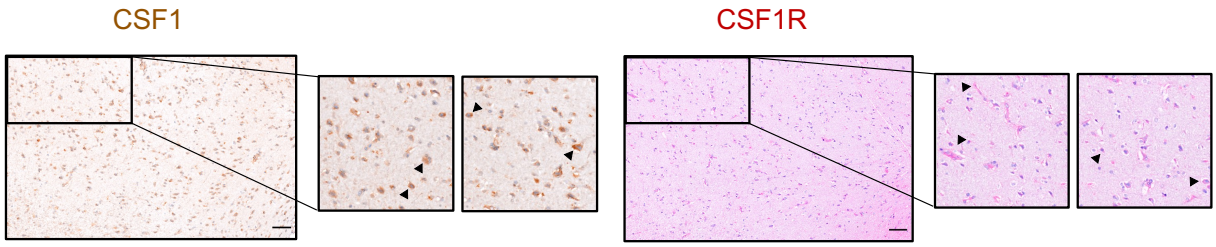
CSF1
CSF1R

C

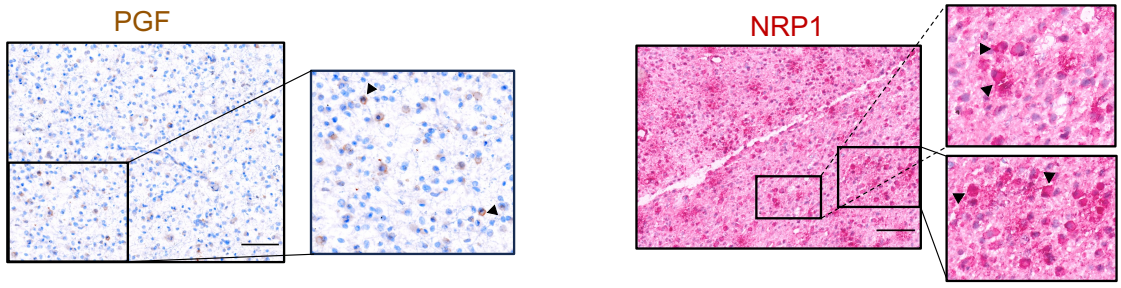
PGF
NRP1

Figure S9. IHC staining for IDH1 R132H, p-STAT1, CSF1, CSF1R, PGF and NRP1 in IDH mutant glioma tissues. Related to Figure 3. (A) Representative double IHC staining for IDH1 R132H and p-STAT1 in grade 3 astrocytomas of four patients. Images were captured at 40x magnification, and crops from each image are shown next to their respective panels. Cells expressing both IDH1 R132H (brown) and p-STAT1 (blue) are indicated by black arrows. Cells expressing only p-STAT1 (blue) are marked by blue arrows, while cells expressing only IDH1 R132H (brown) are indicated by brown arrows. **(B)** Representative IHC staining for CSF1 (brown, left) and CSF1R (red, right) are shown in grade 2 primary astrocytomas. Nuclei are stained blue. Images are taken at 40x magnification, and crops from each image are shown next to their respective panels. Arrows indicate representative stained cells. Scale bar, 100 mm. **(C)** Representative IHC staining for PGF (brown, left) and NRP1 (red, right) are shown in grade 2 astrocytomas. Images are taken at 40x magnification, and crops from each image are shown next to their corresponding panels. Nuclei are stained blue. Arrows indicate representative stained cells. Scale bar, 100 mm.

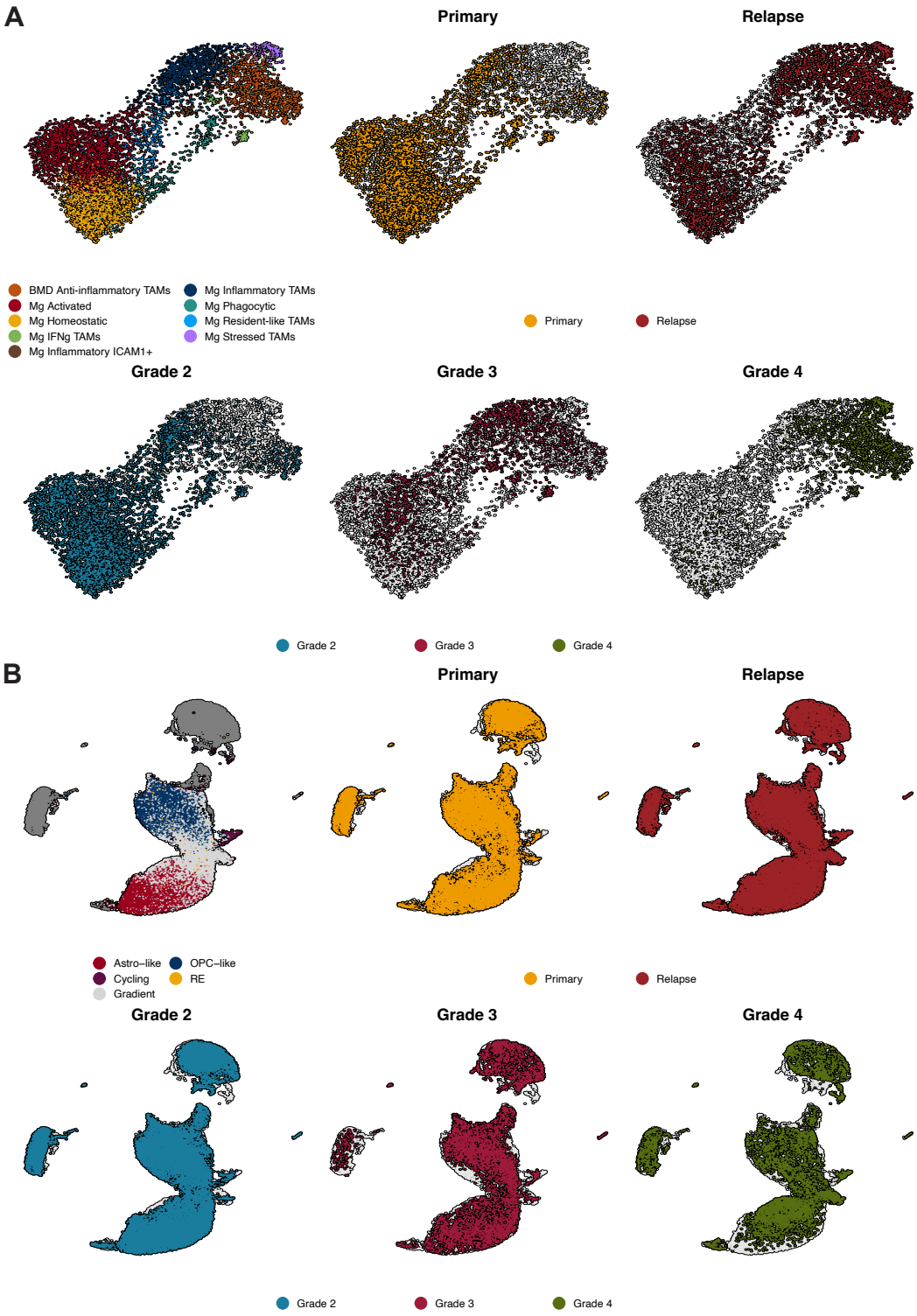

Figure S10. UMAP of integrated TAMs and paired primary-recurrent astrocytomas. Related to Figures 3 and 4. (A) UMAP representation of integrated microglia from astrocytomas and oligodendrogliomas. Colors depict TAM clusters (top left), relapse status (top middle, top right) or grade (bottom). UMAP1, *x*-axis; UMAP2, *y*-axis**. (B)** UMAP representation of paired astrocytomas. Clusters are colored by tumor populations (top left), relapse status (top middle, top right), or grade (bottom). UMAP1, *x*-axis; UMAP2, *y*-axis.